

A Amino acid differences among recombinant input viruses

Pos.	Rn1	A	B	B _{SLIS}
180	Y	L	Y	Y
183	G	G	S	S
184	A	P	T	T
190	T	T	T	S
196	V	F	V	V
199	F	L	I	I
207	T	T	S	S
208	E	R	E	E
212	T	T	A	A
353	V	V	V	L
369	F	F	F	I
422	M	T	M	M
435	P	S	S	S
441	G	E	G	G
458	P	S	P	P
477	T	T	A	A
481	E	K	E	E
500	T	T	A	A
505	R	R	W	W
518	D	N	S	S
550	N	N	N	S
569	L	P	P	P
570	G	G	R	R
572	A	V	A	A
586	L	L	S	S
1397	V	A	V	V
1661	I	I	V	V
2213	D	N	N	N
2214	N	N	K	K
2223	E	E	V	V
2225	Q	R	R	R
2315	M	V	V	V
2575	R	Q	R	R
2586	K	K	N	N
2935	I	I	T	T

B Deep sequencing of input populations

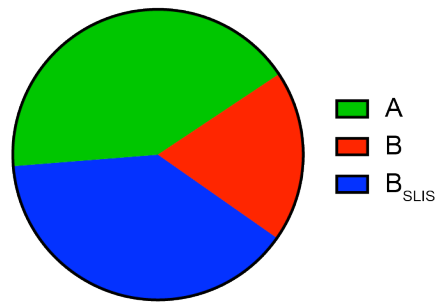


Figure S1. Deep sequencing of recombinant virus populations utilized for *in vivo* studies. . Associated with main Figure 1. **(A)** The amino acid sequence differences for NrHV-A (Genbank: MF113386), NrHV-B (Genbank ON758386) and B_{SLIS} (NrHV-B with the additional changes T190S, V353L, F369I and N550S) as compared to the RHV-rn1 reference isolate (Genbank: KX905133) virus strain. **(B)** Deep sequencing of the input virus pool which revealed a stoichiometry of 42% A, 19% B, 39% B_{SLIS}. Three additional mutations (207T, 1221P and 1590G) were noted in all B virus sequences likely acquired during stock generation *in vivo*.

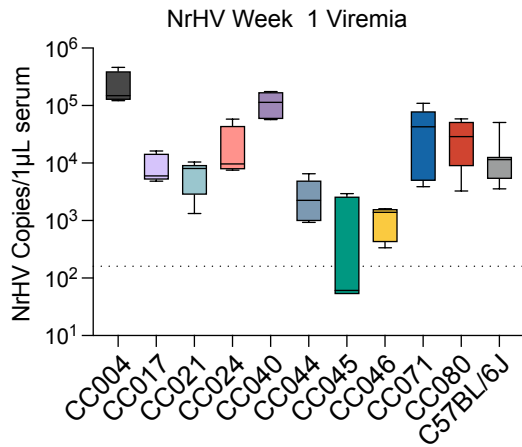


Figure S2. NrHV week 1 viremia for 10-strain Collaborative Cross screen. Associated with main Figure 1. Ten CC strains and control C57BL/6J female mice 9-13 weeks in age were infected with 1×10^5 G.E. of recombinant NrHV or negative control PBS via retroorbital injection and bled weekly to monitor viremia. Infected mouse numbers per strain were: C57BL/6J N = 8, CC004 N = 4, CC017 N = 4, CC021 N = 4, CC024 N = 5, CC040 N = 5, CC044 N = 5, CC045 N = 5, CC046 N = 6, CC071 N = 5, CC080 N = 4. For all strains PBS mock infected N = 3. Levels of viral RNA in 1µl serum as measured by qRT-PCR is shown.

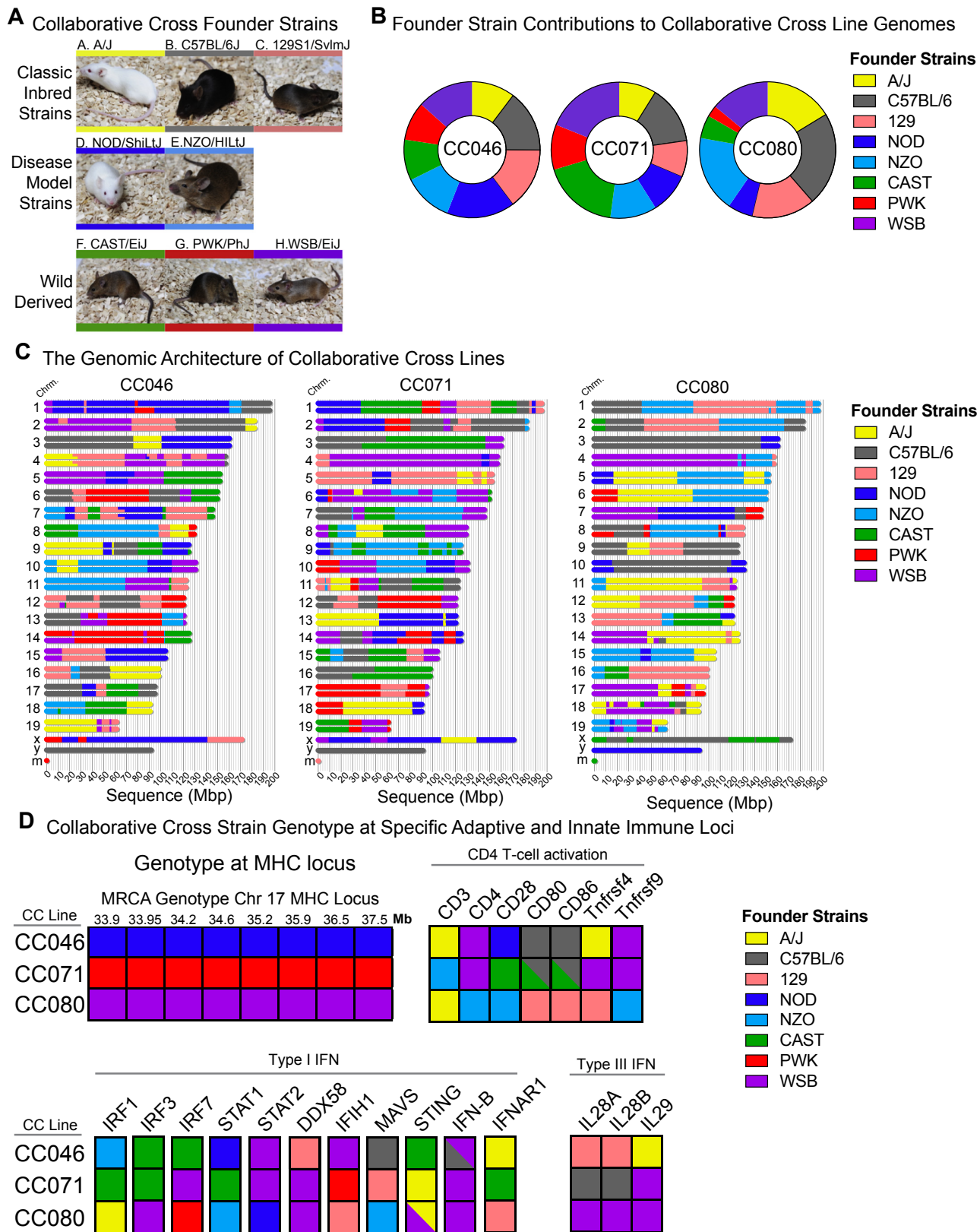


Figure S3. The genetic architecture of Collaborative Cross strains CC046, CC071, and CC080. Associated with main Figure 2. Figure adapted from Leist et al.⁴¹ (A) The CC is a recombinant inbred mouse reference population generated by breeding five classic inbred strains (A/J, C57BL/6, 129, NOD and NZO) with three wild strains (CAST, PWK and WSB). (B) The proportion of each founder strain comprising each CC strain of interest. (C) The genomic architecture of CC046, CC071 and CC080. The color segments of each chromosome pair correspond to loci donated by founder strains. (D) The genotype of CC046, CC071 and CC080 at the MHC locus, genes related to T-cell activation and type I and III interferon. The colors in the grid correspond to the genotype at each region.

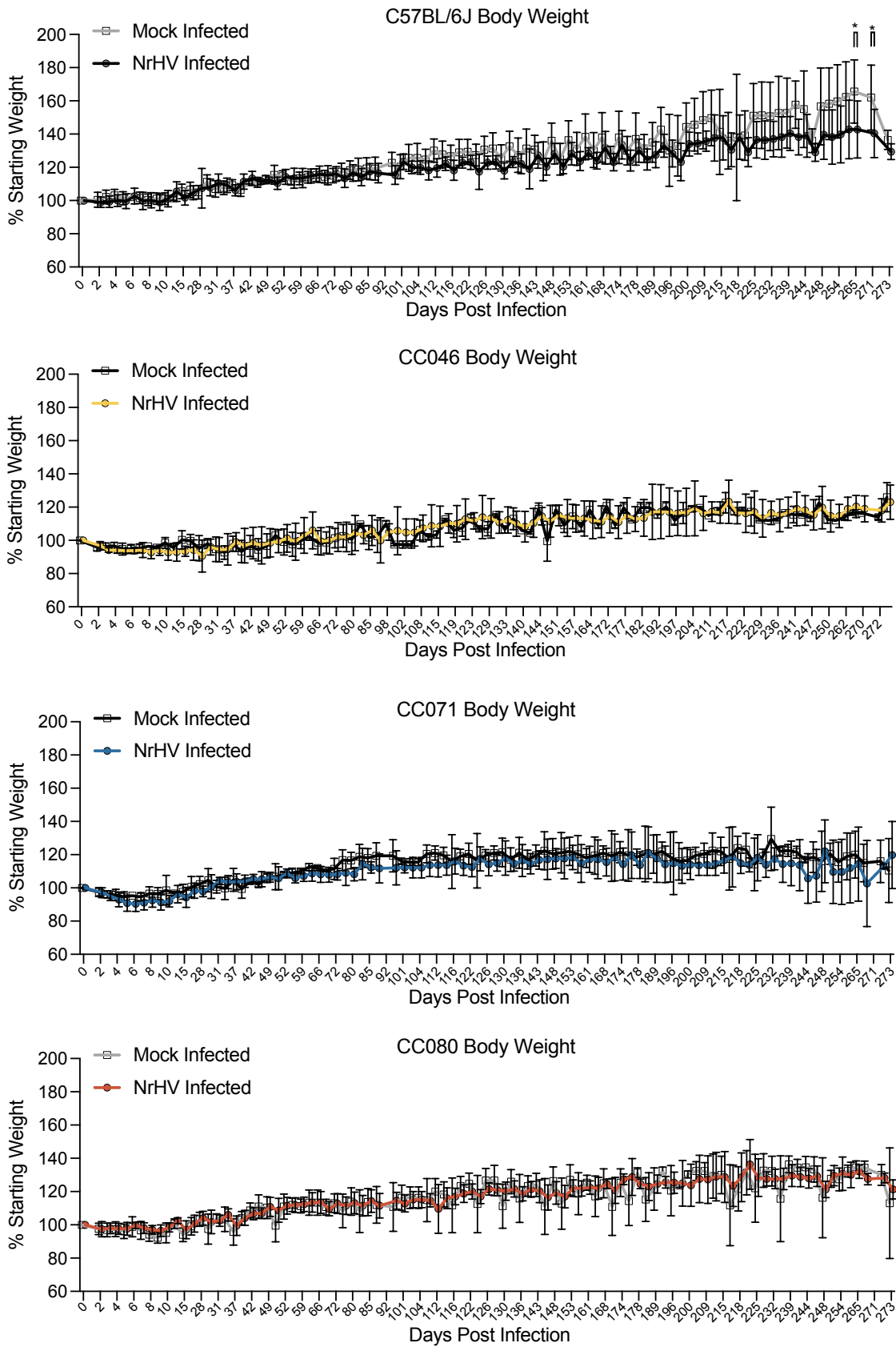


Figure S4. Body weight for mock and NrHV infected mice. Associated with main Figure 2. C57BL/6J, CC046, CC071 and CC080 mice were infected with 1×10^5 G.E. of recombinant NrHV or negative control PBS via retroorbital injection. Body weights were measured daily for the first two weeks and then intermittently for the duration of the study to 272 or 273dpi. The percent starting weight is shown for age and strain matched mock PBS infected and NrHV infected over time.

Body Weight (Week 1-2)

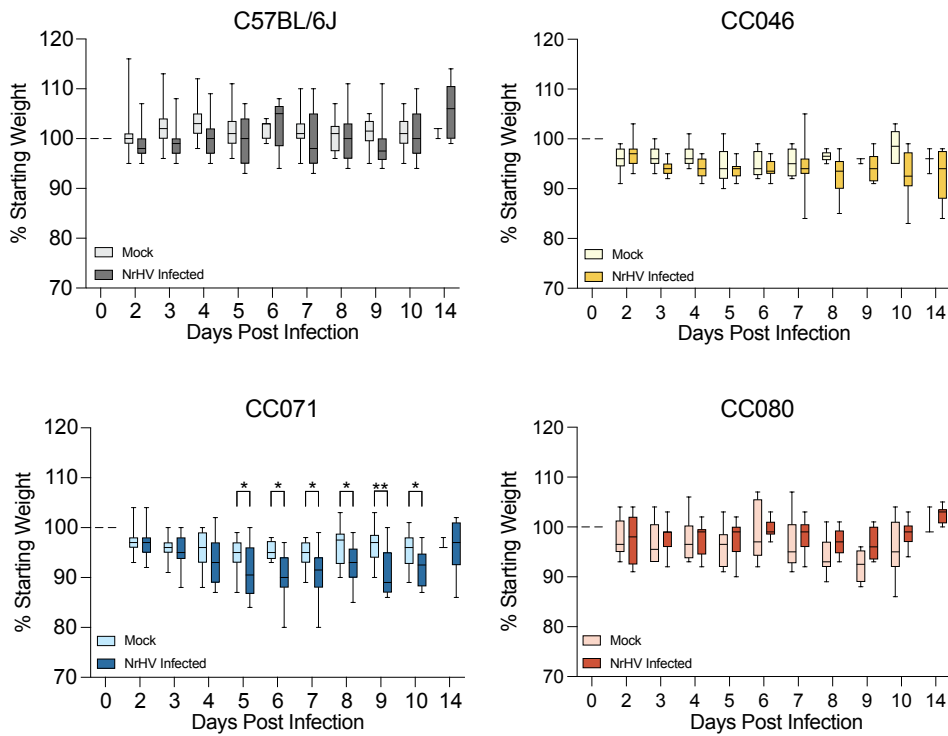


Figure S5. Body weight for mock and NrHV infected mice for days 0-14. Associated with main Figure 2 and Figure S4. C57BL/6J, CC046, CC071 and CC080 mice were infected with 1×10^5 G.E. of recombinant NrHV or negative control PBS via retroorbital injection. Daily body weights are shown for the first 14 days of infection. Asterisks indicate statistical significance by two-way ANOVA with a Sidak's multiple comparison test.

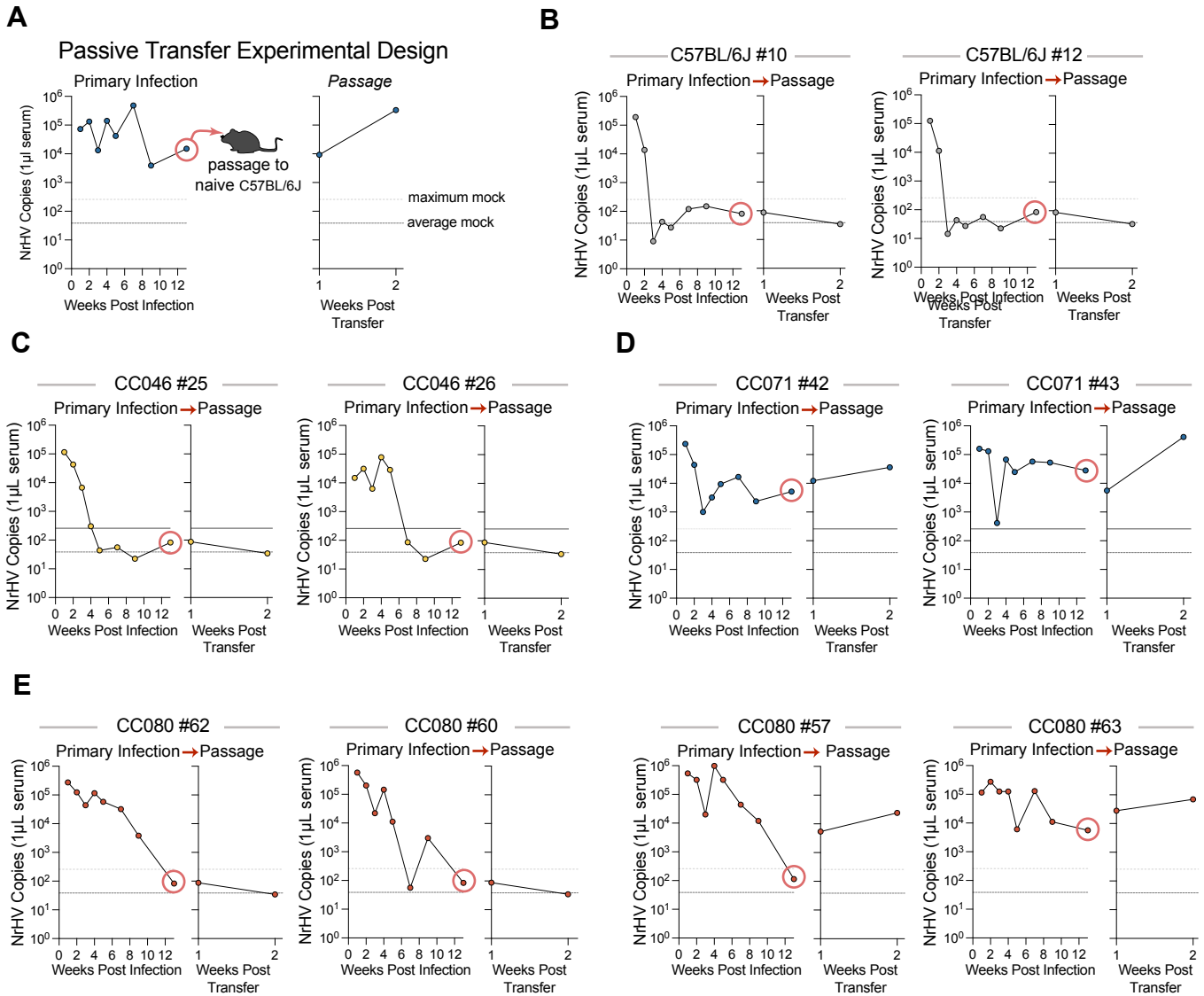


Figure S6. Passive transfer to demonstrate the presence of infectious virus. Associated with main Figure 2. **(A)** To demonstrate the presence of infectious virus in NrHV RNA positive sera, 5µl of serum from 12 weeks post infection was diluted in 150µl PBS and 100µl of this mixture was used to inoculate naïve C57BL/6J mice via the retroorbital route. **(B)** Transfer of serum from previously infected aviremic C57BL/6J mice to recipient naïve C57BL/6J mice. **(C)** Transfer of serum from previously infected but aviremic CC046 mice to recipient naïve C57BL/6J mice. **(D)** Transfer of serum from viremic CC071 mice to recipient naïve C57BL/6J mice. **(E)** Transfer of serum from three aviremic mice and one viremic CC080 mouse to three recipient naïve C57BL/6J mice.

Kinetics of viremia per mouse per mouse strain

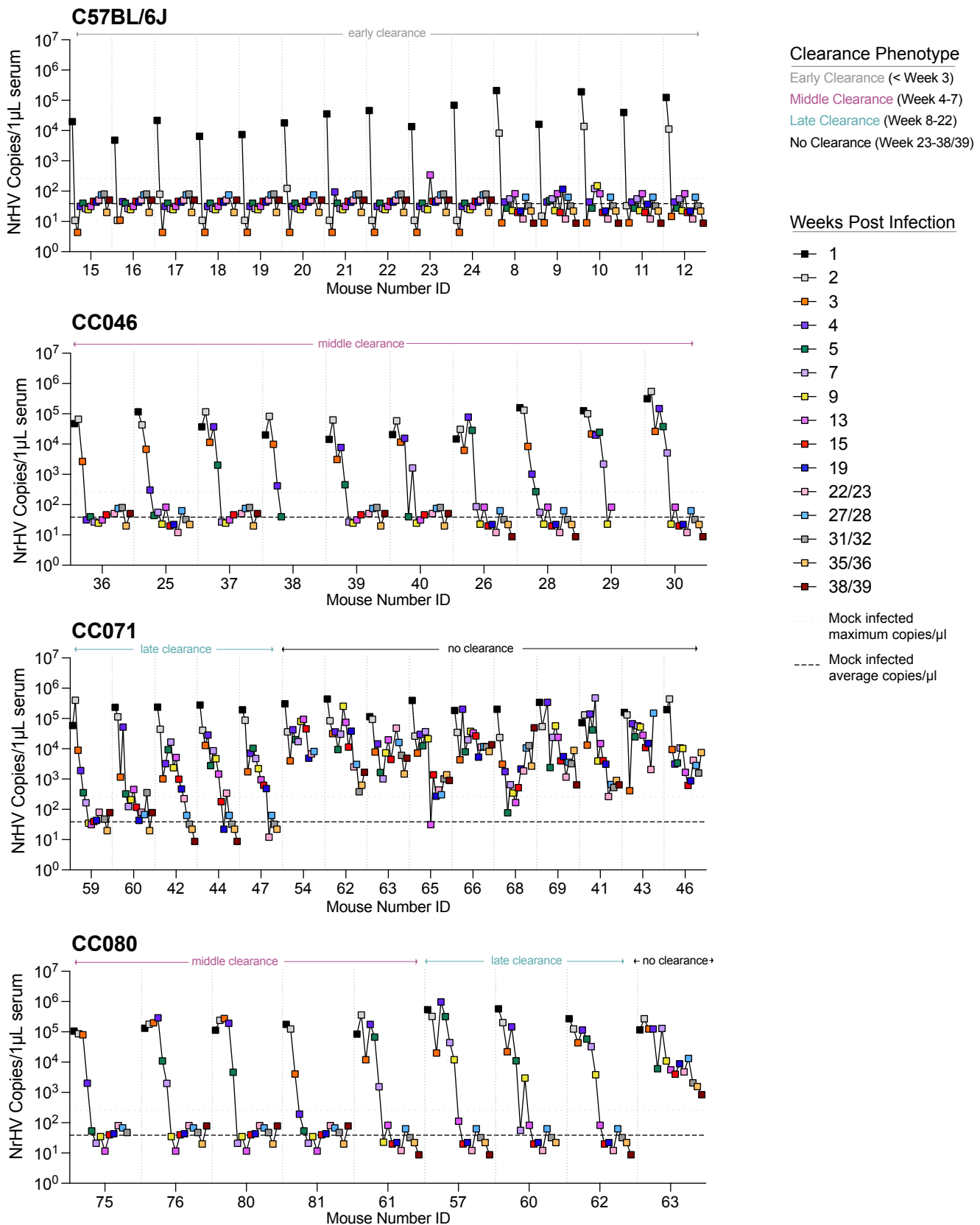
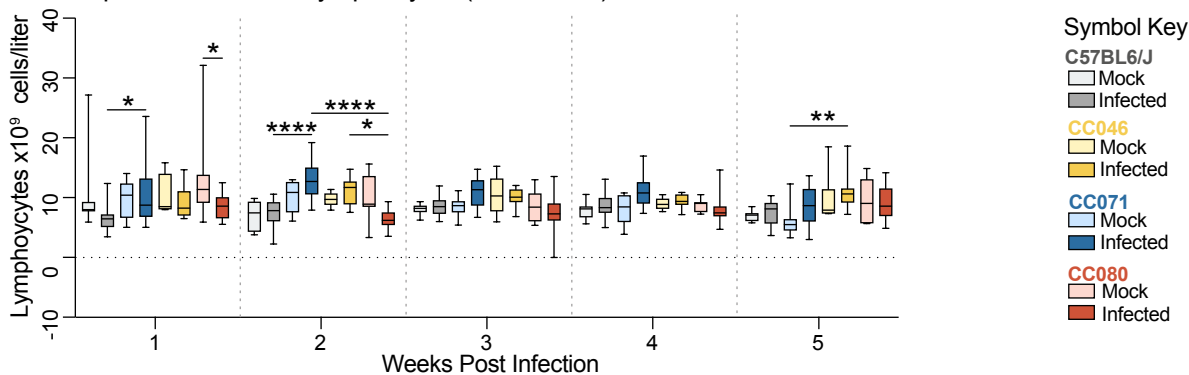
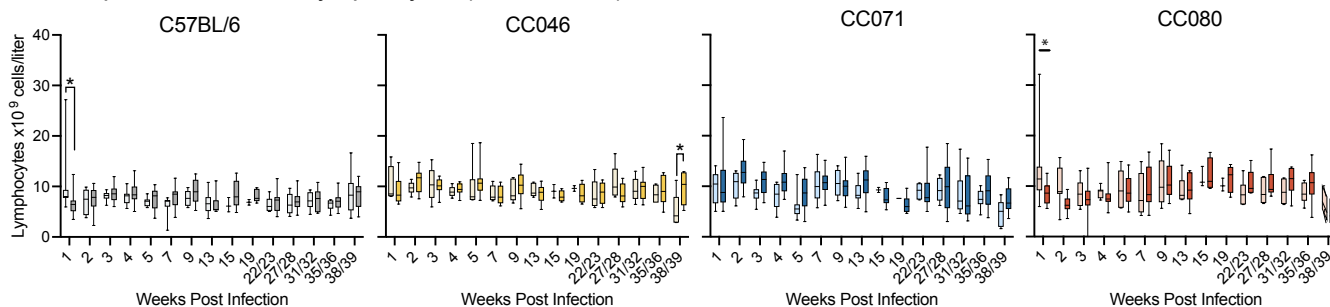


Figure S7. Kinetics of viremia in individual mice with different viral clearance phenotypes. Associated with main Figure 2. The levels of viral RNA in serum as measured by qRT-PCR are shown for C57BL/6J, CC046, CC071 and CC080. Four clearance phenotypes were noted: Early Clearance (< 3 weeks), Middle Clearance (Week 4-7), Late Clearance (Week 8-22), No Clearance (viremic at the end of study week 38/39).

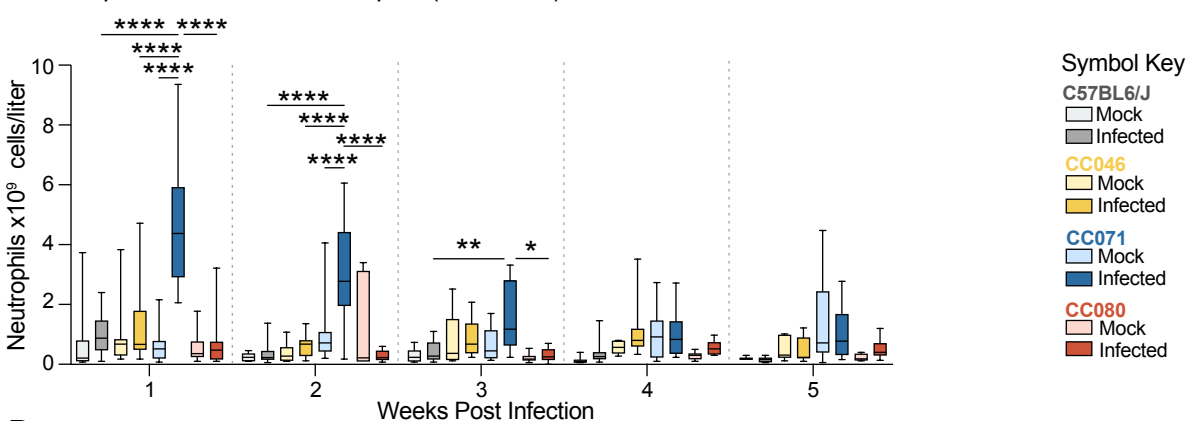
A Complete Blood Count: Lymphocytes (Weeks 1-5)



B Complete Blood Count: Lymphocytes (Weeks 1-39)



C Complete Blood Count: Neutrophils (Weeks 1-5)



D Complete Blood Count: Neutrophils (Weeks 1-39)

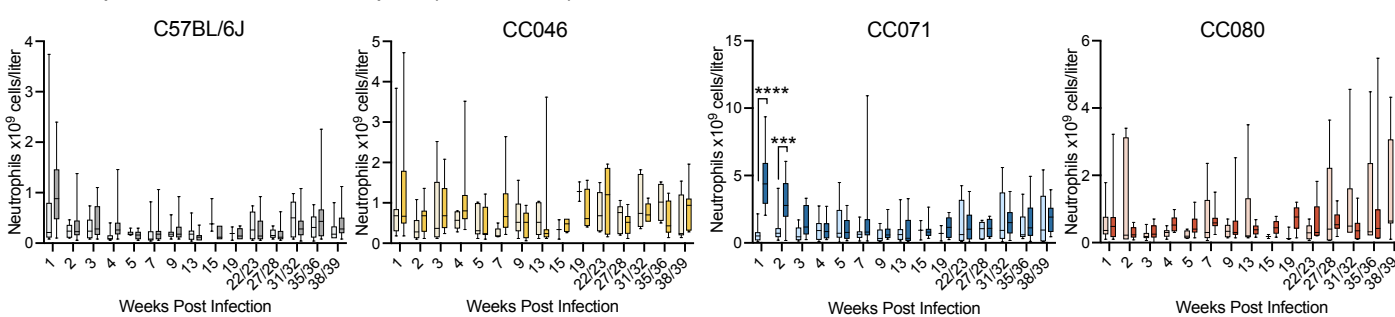


Figure S8. Total blood lymphocytes and neutrophils for all times post infection. Associated with main Figure 4. Complete blood count was performed using a Vetscan HM5 automated blood analyzer on whole blood isolated from mock and infected mice for the duration of studies described in Fig. 2. **(A)** Blood lymphocytes are shown for the first five weeks of infection or **(B)** for the duration of the study for each mouse strain. **(C)** Complete blood count for neutrophils for the first five weeks of infection or **(D)** for the duration of the study for each mouse strain. Asterisks indicate statistically significant differences by Two-Way ANOVA Tukey's multiple comparisons test.

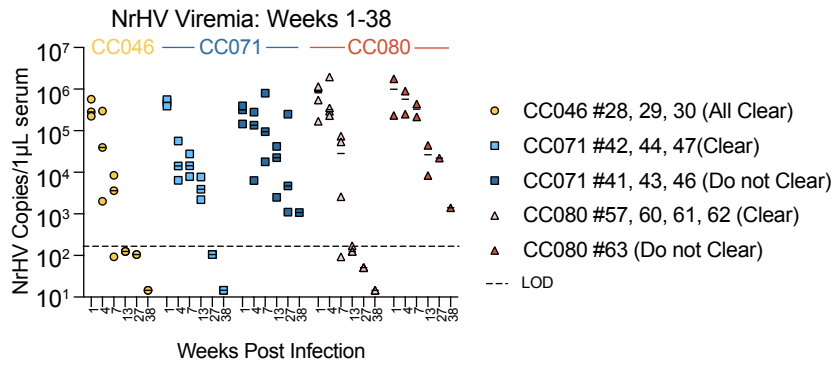


Figure S9. Viremia phenotypes for mice on which viral ORF sequencing was performed. Associated with main Figure 6 and Figure S12. The levels of viral RNA in serum as measured by qRT-PCR are shown for C57BL/6J, CC046, CC071 and CC080.

A

Dendrogram (NrHV genome)

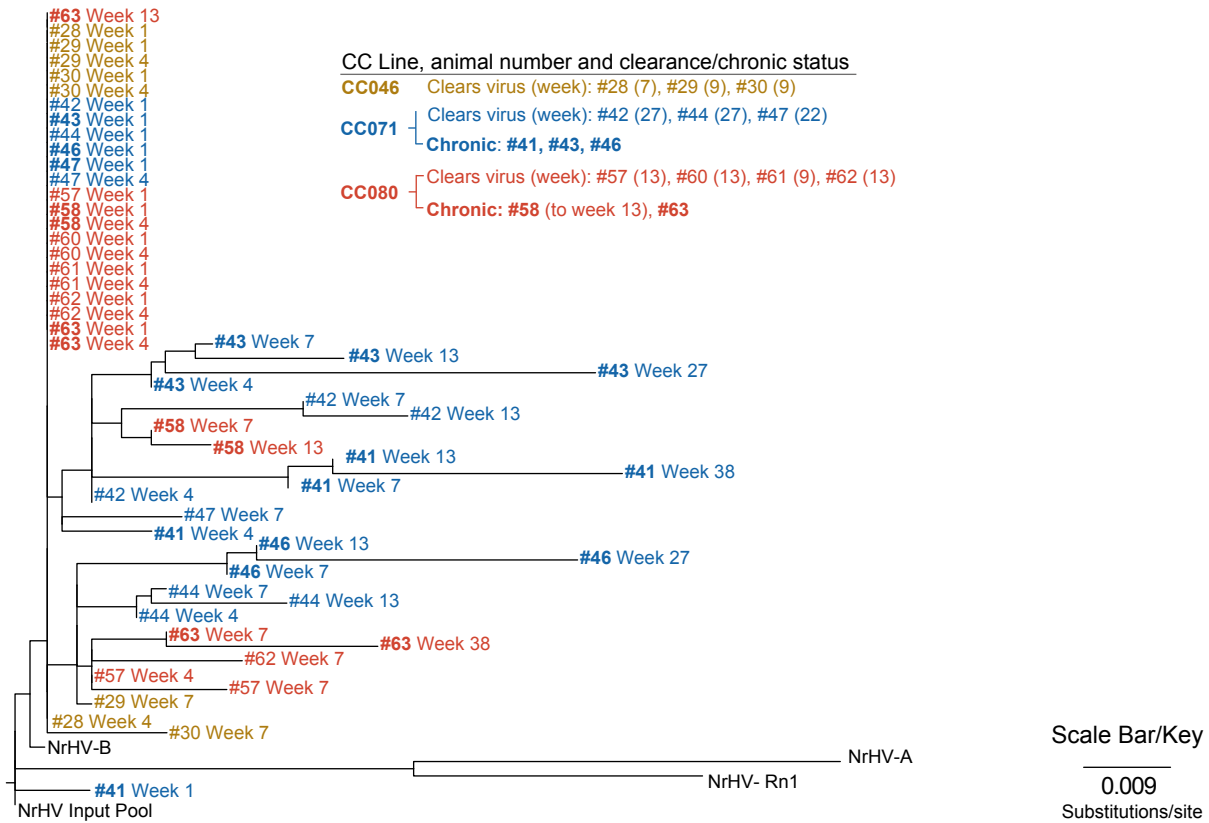
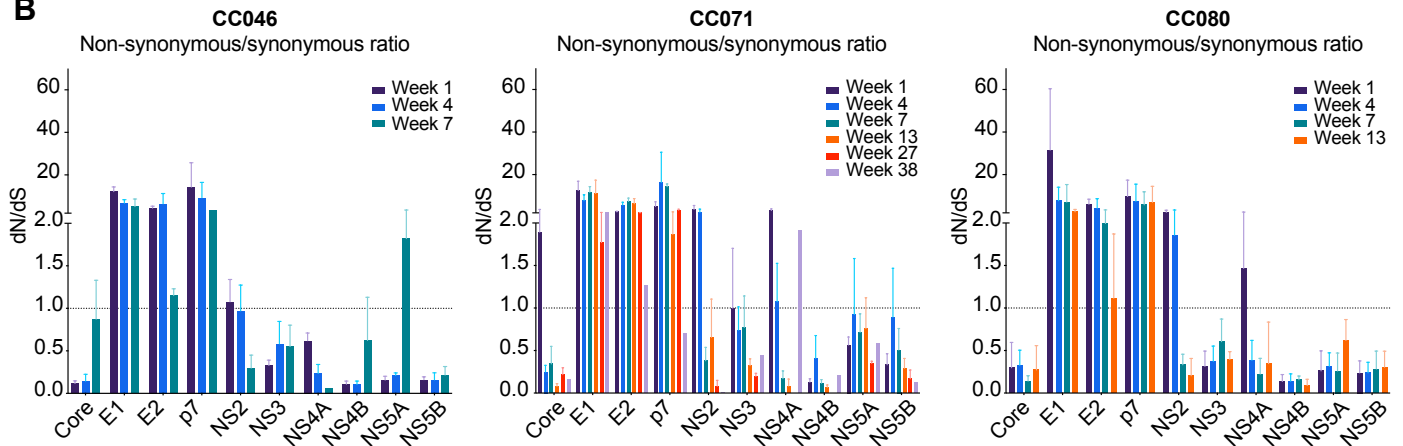
**B**

Figure S10. Chronic infection is associated with increased viral evolution. (A) Associated with main Figure 6 and Figure S9. The genetic relationships of virus populations isolated from NrHV infected CC046 (N = 3), CC071 (N = 6) or CC080 (N = 6) over time are shown in a neighbor joining tree created from whole viral ORF sequences from 1, 4, 7, 13, 27 and 38 weeks post infection. Infected animals and phenotypes are described in Figure 2. The viremia phenotypes per mouse are described in Figure S9. The dendrogram was generated by aligning full ORF sequences by MAFFT and building the phylogeny by maximum likelihood using PhyML using the general time reversible substitution model and rooted the inoculum input of the current study and the rat inoculum used for NRG mouse adaptation (NrHV-A; Genebank MF113386)¹³, NrHV-B (Genebank ON758386)¹³ and RHV-rn1 (Genebank KX905133)⁹ as outgroups. (B) Non-synonymous/synonymous (dN/dS) mutation ratios. Using whole ORF sequencing data from (A), dN/dS ratios were generated for each viral protein. Increased dN/dS is associated with increased evolutionary change.

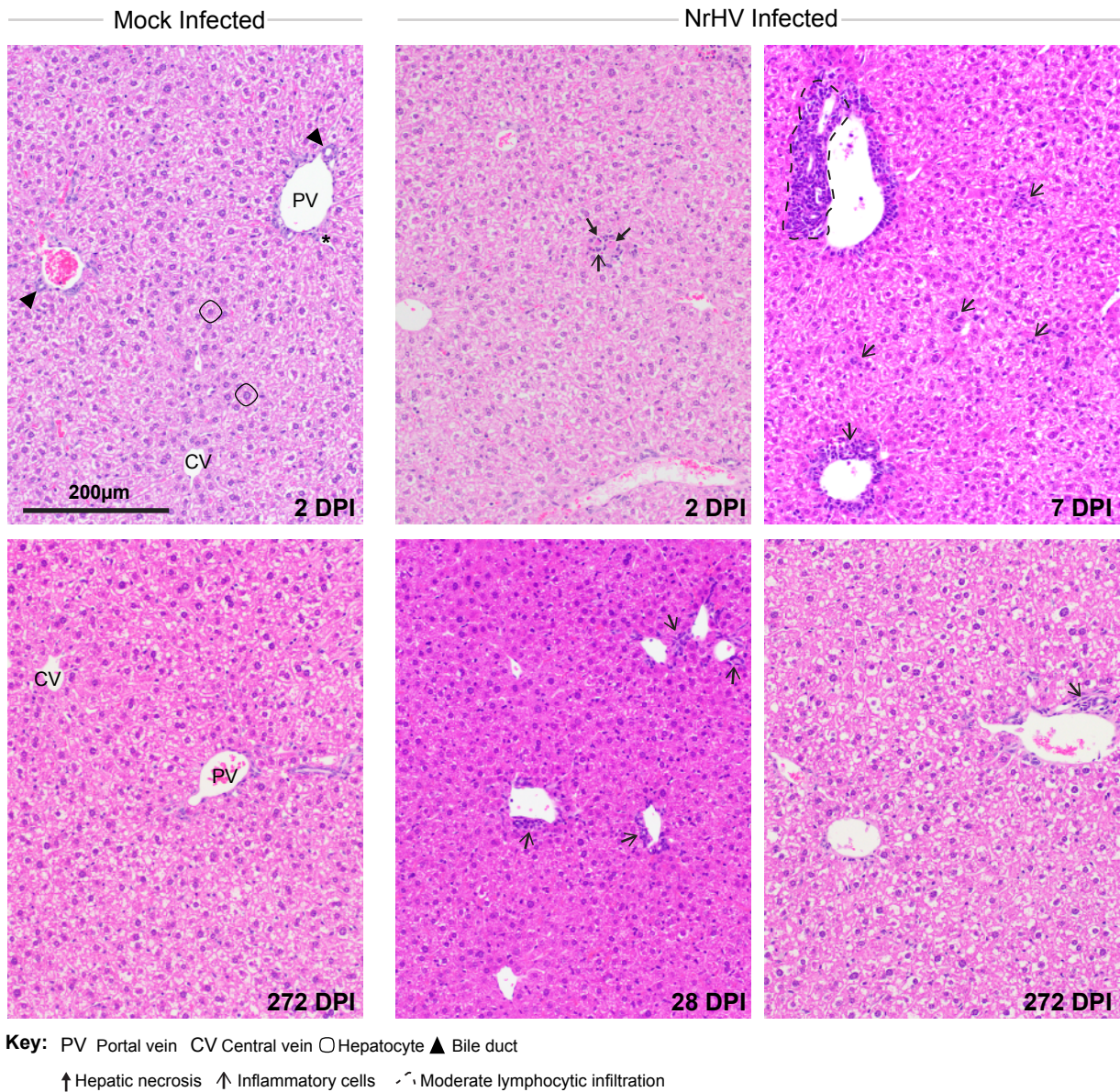


Figure S11. Liver pathology in mock and NrHV infected WT C57BL/6J mice. Liver tissue sections from mock or NrHV infected mice at 2, 7, 28 and 272 dpi were stained with hematoxylin and eosin. Hallmark features of normal liver architecture including portal vein, bile duct, hepatic artery, central vein and hepatocytes are noted in each mock panel. Other pathologic features are noted in the key.

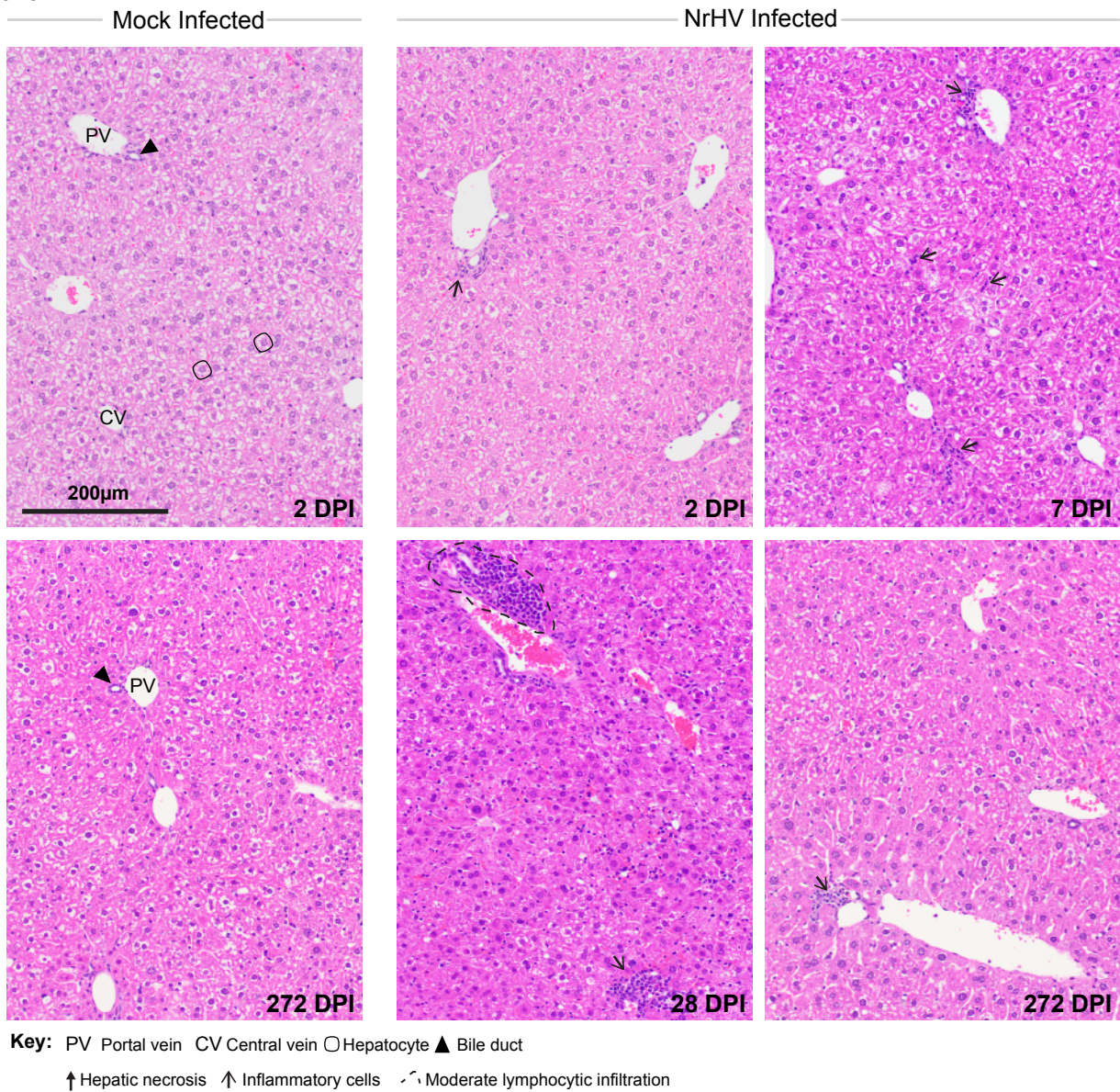
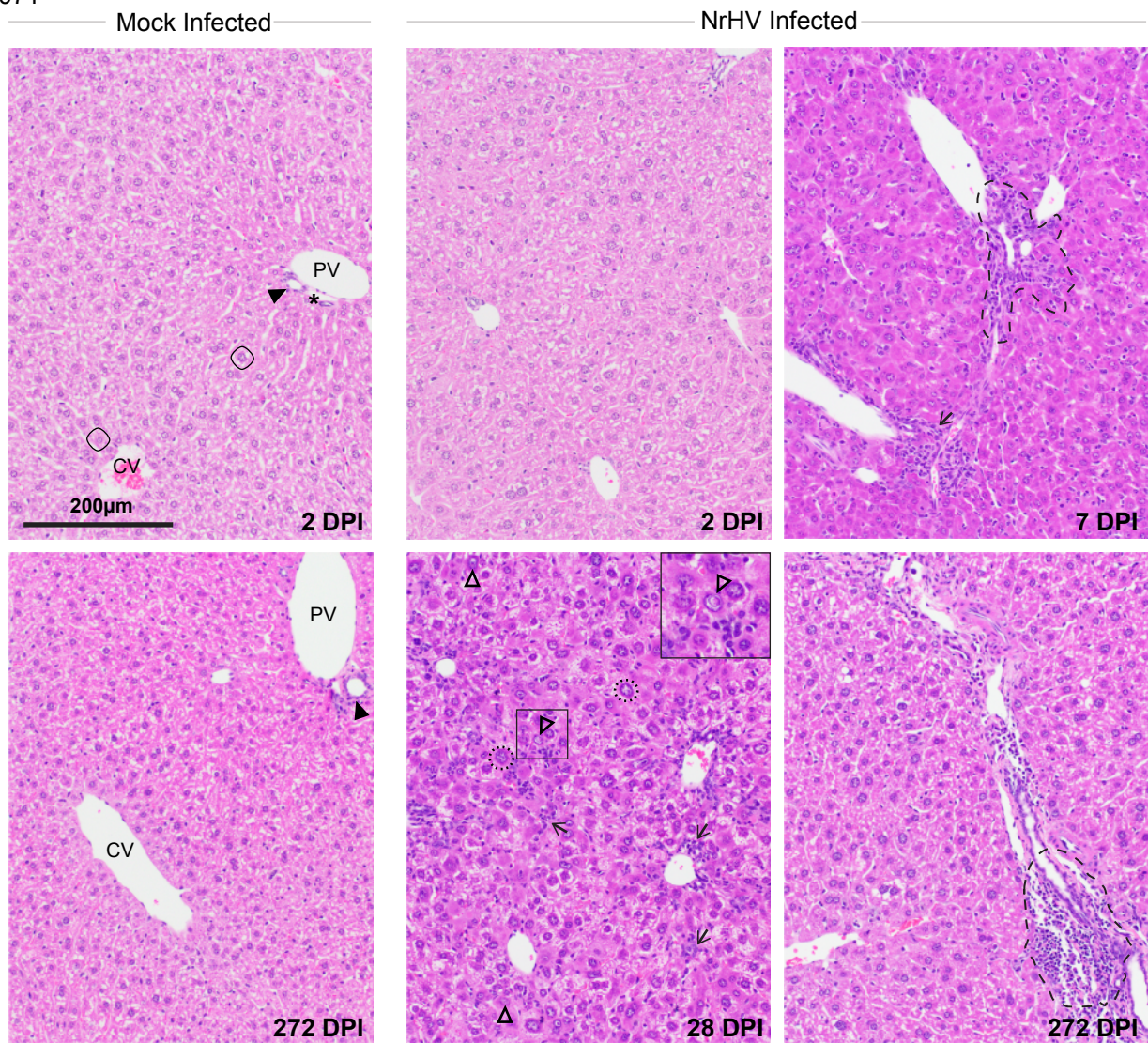
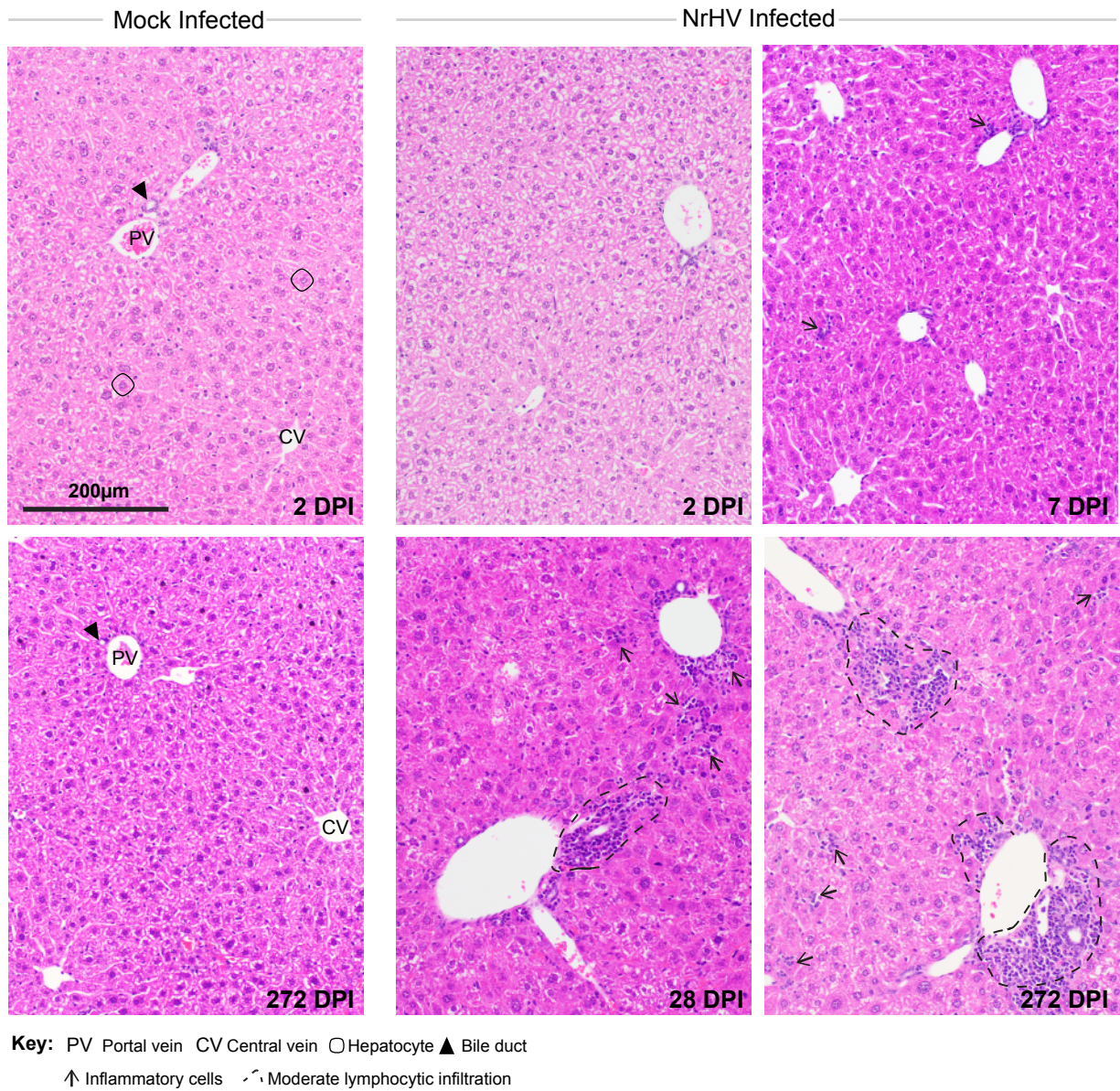


Figure S12. Liver pathology in mock and NrHV infected CC046 mice. Liver tissue sections from mock or NrHV infected mice at 2, 7, 28 and 272 dpi were stained with hematoxylin and eosin. Hallmark features of normal liver architecture including portal vein, bile duct, hepatic artery, central vein and hepatocytes are noted in each mock panel. Other pathologic features are noted in the key.



Key: PV Portal vein CV Central vein * Hepatic artery ○ Hepatocyte ▲ Bile duct ⦿ Karyomegaly
 ↑ Hepatic necrosis △ Hepatocyte nuclear inclusions ↗ Inflammatory cells ⦶ Moderate lymphocytic infiltration

Figure S13. Liver pathology in mock and NrHV infected CC071 mice. Liver tissue sections from mock or NrHV infected mice at 2, 7, 28 and 272 dpi were stained with hematoxylin and eosin. Hallmark features of normal liver architecture including portal vein, bile duct, hepatic artery, central vein and hepatocytes are noted in each mock panel. Other pathologic features are noted in the key.



Key: PV Portal vein CV Central vein ○ Hepatocyte ▲ Bile duct
 ↑ Inflammatory cells - - - Moderate lymphocytic infiltration

Figure S14. Liver pathology in mock and NrHV infected CC080 mice. Liver tissue sections from mock or NrHV infected mice at 2, 7, 28 and 272 dpi were stained with hematoxylin and eosin. Hallmark features of normal liver architecture including portal vein, bile duct, hepatic artery, central vein and hepatocytes are noted in each mock panel. Other pathologic features are noted in the key.

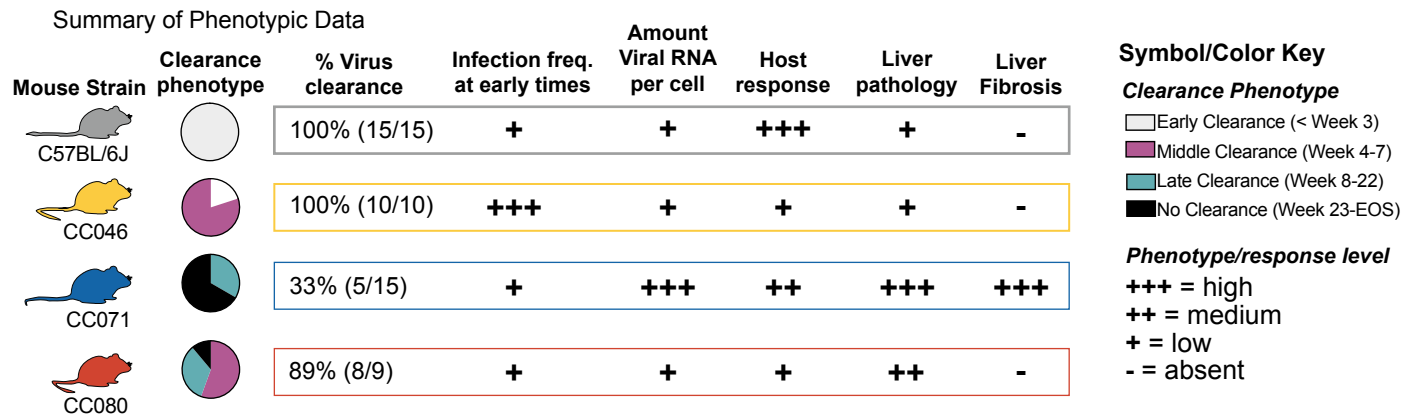


Figure S15. Summary of key phenotypic data per mouse strain. Key phenotypic data per mouse strain is shown to provide an overview of the main pieces of data described in the manuscript.